Proceedings of the Institute of Acoustics

PARABOLIC EQUATION TECHNIQUES IN OCEAN ACOUSTICS

Michael D. Collins

Naval Research Laboratory, Washington, DC 20375, USA

1. INTRODUCTION

The parabolic equation (PE) method [1,2] is an efficient approach for solving range-dependent ocean acoustics problems [3] that is based on the limit of an outgoing wave propagating nearly horizontally in a nearly homogeneous medium. This paper describes recent improvements in the accuracy, capability, and efficiency of the PE method. Sections 2-7 summarize previously published results and provide references that contain examples. Sections 8-11 describe unpublished results and contain examples. The higher-order PE (Section 2) is accurate for problems involving nearly vertical propagation and large variations in the properties of the medium [4,5]. With energy-conservation corrections (Section 3), the PE method is accurate for range-dependent problems [6-8]. The two-way PE (Section 4) may be used to solve some back-scattering problems [9,10]. The elastic PE (Section 5) handles problems involving interaction with an elastic ocean bottom [11-14]. The split-step Padé solution (Section 6) is orders of magnitude faster than standard numerical techniques for solving the higher-order PE and the elastic PE [15,16]. The self-starter (Section 7) is an accurate and efficient technique for generating initial conditions [17]. The poro-elastic PE (Section 8) handles problems involving interaction with a poro-elastic ocean bottom [18]. The adiabatic mode PE (Section 9) is an efficient approach for solving three-dimensional problems [19,20]. The windy PE (Section 10) is a generalization of the adiabatic mode PE for problems involving fluid flow that has been applied to model sound propagation from the impact sites of the fragments of Comet Shoemaker-Levy 9 [21]. The PE method has been extended to handle problems involving waveguides of variable thickness (Section 11) and used to solve beach acoustics problems [22].

2. THE HIGHER-ORDER PE

We work in cylindrical coordinates, where z is the depth below the ocean surface, the range r is the horizontal distance from a time-harmonic point source at $z = z_0$, and θ is the azimuth. We remove the spreading factor $r^{-1/2}$ and the time dependent factor $\exp(-i\omega t)$ from the complex pressure p, where t is time and ω is the circular frequency of the source. The environment is approximated by a set of regions in which the acoustic parameters, the wave number k and the density ρ, depend only on z. In Section 3, we describe an accurate approach for treating the vertical interfaces between regions. The farfield wave equation,

$$\frac{\partial^2 p}{\partial r^2} + \frac{1}{r^2}\frac{\partial^2 p}{\partial \theta^2} + \rho \frac{\partial}{\partial z}\left(\frac{1}{\rho}\frac{\partial p}{\partial z}\right) + k^2 p = 0 , \tag{2.1}$$

is valid in each of the stratified regions.

The second term in (2.1) may be neglected for many problems in ocean acoustics [23]. Since it is rarely practical to perform three-dimensional calculations, the uncoupled azimuth approximation is one of the most important approximations in ocean acoustics. Although the uncoupled azimuth solution is obtained by solving the two-dimensional wave equation,

$$\frac{\partial^2 p}{\partial r^2}+\rho\frac{\partial}{\partial z}\left(\frac{1}{\rho}\frac{\partial p}{\partial z}\right)+k^2 p=0\,, \tag{2.2}$$

this solution is three dimensional if k and ρ depend on θ. We describe an efficient approach for handling azimuthal coupling in Section 9.

Rearranging (2.2), we obtain

$$\frac{\partial^2 p}{\partial r^2}+k_0^2(1+X)p=0\,, \tag{2.3}$$

$$X=k_0^{-2}\left(\rho\frac{\partial}{\partial z}\frac{1}{\rho}\frac{\partial}{\partial z}+k^2-k_0^2\right), \tag{2.4}$$

where k_0 is a representative wave number. Factoring the operator in (2.3) into incoming and outgoing operators, we obtain

$$\left(\frac{\partial}{\partial r}+ik_0\sqrt{1+X}\right)\left(\frac{\partial}{\partial r}-ik_0\sqrt{1+X}\right)p=0\,. \tag{2.5}$$

We remove the factor $\exp(ik_0 r)$ from p and assume that incoming energy is dominated by outgoing energy to obtain the outgoing wave equation,

$$\frac{\partial p}{\partial r}=ik_0\left(-1+\sqrt{1+X}\right)p\,. \tag{2.6}$$

An approach for treating incoming energy is described in Section 4. The outgoing wave equation is solved by approximating the square-root function for small X. The linear approximation that was used in the original ocean acoustics PE [3] is restricted to problems involving nearly horizontal propagation and small variations in the acoustic parameters. A rational-linear approximation [24] was later implemented to achieve improved accuracy [25,26]. An arbitrary level of accuracy may be achieved by using an n-term rational approximation to obtain the higher-order PE,

$$\frac{\partial p}{\partial r}=ik_0\sum_{j=1}^{n}a_{j,n}\left(1+b_{j,n}X\right)^{-1}Xp\,. \tag{2.7}$$

The coefficients $a_{j,n}$ and $b_{j,n}$ are selected so that the PE is accurate and stable. The coefficients given by analytic expressions in [4] provide accuracy in a wide region about $X = 0$. The coefficients tabulated in [14], which provide accuracy and annihilate the evanescent spectrum, are useful for problems involving energy-conservation corrections (Section 3) and required for problems involving elastic layers (Section 5). The higher-order PE is solved using standard numerical techniques [5].

3. ENERGY-CONSERVATION CORRECTIONS

The quantities p and $\rho^{-1}\,\partial p/\partial r$ are conserved across the vertical interfaces between range-independent regions. Since the outgoing wave equation involves only one range derivative, it is not possible for the PE solution to satisfy both of these conditions. For weak range dependence, it is often possible to achieve accurate results by conserving p and ignoring the other condition. This approach was used in PE algorithms until it became evident that amplitude errors of several decibels can arise for problems involving sloping ocean bottoms [6,27]. A high level of accuracy may be achieved for range-dependent problems by conserving energy flux across the vertical interfaces. Although this approach involves only one condition, it was not successfully implemented until two difficulties were resolved.

One of the difficulties is the fact that conserving the energy flux,

$$E = \int \frac{p}{\rho}\frac{\partial p}{\partial r}\,dz\,, \tag{3.1}$$

is a nonlinear condition (note that E is conserved if both p and $\rho^{-1}\,\partial p/\partial r$ are conserved). This difficulty was resolved for coupled-mode solutions by replacing conservation of E with conservation of $\rho^{-1/2}p$ [6]. This linear condition is a good approximation of conservation of E if the horizontal wave-number spectrum is narrow and $\partial p/\partial r \cong ik_0 p$.

The other difficulty is that severe Gibbs oscillations arise when energy-conservation corrections are implemented into PE solutions (the coupled-mode solution is immune to this problem). This difficulty was resolved by using a rational approximation (Section 2) that annihilates the evanescent spectrum [7]. The results in [7] indicate that conserving $(\rho c)^{-1/2}p$ rather than $\rho^{-1/2}p$ provides greater accuracy. Benchmark tests indicate that this partial correction provides accurate solutions for most range-dependent problems in ocean acoustics.

The complete energy-conservation correction [8] is based on conserving the quantity,

$$A = \rho^{-1/2}(1+X)^{1/4}\,p\,, \tag{3.2}$$

across vertical interfaces. The fourth root of the operator in (3.2) is approximated using rational functions. By expressing p in terms of normal modes and using the properties of the normal modes, we obtain

$$E = \int A^2 \, dz. \tag{3.3}$$

Benchmark tests involving sediment sound speeds as high as 5000 m / s indicate that the complete energy-conservation correction is accurate for the most extreme range-dependent problems for which outgoing energy dominates back-scattered energy. For the acoustic case, the complete correction is of limited practical importance because the partial correction is robust. A complete correction for the elastic case would be very useful, however, because the partial correction is not robust for the elastic case [8].

4. THE TWO-WAY PE

The PE method can be used to solve back-scattering problems [9,10]. The single-scattering approximation [28] is applied at the vertical interfaces between regions. The PE method is used to eliminate range derivatives from one of the interface conditions to obtain a boundary-value problem for the scattered field. A related approach has been used to solve other scattering problems [29,30].

The following conditions hold at a vertical interface between regions A and B:

$$p_i + p_r = p_t, \tag{4.1}$$

$$\frac{1}{\rho_A}\frac{\partial}{\partial r}(p_i + p_r) = \frac{1}{\rho_B}\frac{\partial p_t}{\partial r}, \tag{4.2}$$

where the subscripts A and B denote evaluation in the respective regions and the subscripts i, r, and t denote the incident, reflected, and transmitted fields. From (2.6) and (4.2), we obtain

$$\frac{1}{\rho_A} N_A (p_i - p_r) = \frac{1}{\rho_B} N_B p_t, \tag{4.3}$$

where $N = \sqrt{1+X}$. The minus sign in (4.3) accounts for the fact that p_r is incoming. Using (4.1) to eliminate p_t from (4.3), we obtain

$$\left(\frac{1}{\rho_A} N_A + \frac{1}{\rho_B} N_B\right) p_r = \left(\frac{1}{\rho_A} N_A - \frac{1}{\rho_B} N_B\right) p_i. \tag{4.4}$$

The direct numerical solution of (4.4) involves the solution of a non-banded system of equations. Rearranging (4.4), we obtain the iteration formula,

$$p_r = \left(1 - N_B^{-1} \frac{\rho_B}{\rho_A} N_A\right)\left(\frac{p_r - p_i}{2}\right). \tag{4.5}$$

The numerical solution associated with (4.5) involves the solution of banded systems of equations and converges rapidly if the change in the acoustic parameters across the interface is small. An improved iteration formula is given in [9]. The two-way PE has been generalized to handle some problems involving elastic layers [10].

5. THE ELASTIC PE

It is sometimes necessary to model the ocean bottom as an elastic medium. In this section, we derive the elastic PE for the uncoupled azimuth problem. For simplicity, we work in Cartesian coordinates, where x is the horizontal distance from a line source and y is the other horizontal coordinate. The point source case is easily obtained by modifying the source condition (Section 7) and including cylindrical spreading. It is necessary to use a non-standard formulation of elasticity so that the equations of motion may be factored [11]. It is necessary to use special coefficients for the rational approximation to obtain a stable solution [13].

We derive the equations of motion for a stratified medium using the approach of [31], which involves applying Newton's law $\mathbf{F} = m\mathbf{a}$ to a small volume element. The x and z components of $\mathbf{F} = m\mathbf{a}$ are

$$\frac{\partial \sigma_{xx}}{\partial x} + \frac{\partial \sigma_{xz}}{\partial z} = \rho \frac{\partial^2 u}{\partial t^2}, \tag{5.1}$$

$$\frac{\partial \sigma_{xz}}{\partial x} + \frac{\partial \sigma_{zz}}{\partial z} = \rho \frac{\partial^2 w}{\partial t^2}, \tag{5.2}$$

where $\mathbf{u} = (u,v,w)$ is the displacement vector and σ_{xx}, σ_{xz}, and σ_{zz} are the stresses. The constitutive equations (Hooke's law) are

$$\sigma_{xx} = \lambda\Delta + 2\mu \frac{\partial u}{\partial x}, \tag{5.3}$$

$$\sigma_{xz} = \mu\left(\frac{\partial u}{\partial z} + \frac{\partial w}{\partial x}\right), \tag{5.4}$$

$$\sigma_{zz} = \lambda\Delta + 2\mu \frac{\partial w}{\partial z}, \tag{5.5}$$

where λ and μ are the Lamé constants and $\Delta = \nabla \cdot \mathbf{u}$.

Substituting the constitutive equations into (5.1) and (5.2), we obtain the equations of motion,

$$\mu\frac{\partial^2 u}{\partial x^2}+\mu\frac{\partial^2 u}{\partial z^2}+\rho\omega^2 u+(\lambda+\mu)\frac{\partial\Delta}{\partial x}+\frac{\partial\mu}{\partial z}\frac{\partial u}{\partial z}+\frac{\partial\mu}{\partial z}\frac{\partial w}{\partial x}=0\,, \tag{5.6}$$

$$\mu\frac{\partial^2 w}{\partial x^2}+\mu\frac{\partial^2 w}{\partial z^2}+\rho\omega^2 w+(\lambda+\mu)\frac{\partial\Delta}{\partial z}+\frac{\partial\lambda}{\partial z}\Delta+2\frac{\partial\mu}{\partial z}\frac{\partial w}{\partial z}=0\,. \tag{5.7}$$

The equations of motion are valid for problems involving piece-wise continuous depth variations in the elastic parameters and may be applied to problems involving fluid layers by implementing the interface conditions described in [11,14]. Differentiating (5.6) with respect to x and (5.7) with respect to z and summing, we obtain

$$(\lambda+2\mu)\frac{\partial^2\Delta}{\partial x^2}+\frac{\partial}{\partial z}\left[(\lambda+2\mu)\frac{\partial\Delta}{\partial z}\right]+\rho\omega^2\Delta+$$
$$2\frac{\partial\mu}{\partial z}\frac{\partial^2 w}{\partial x^2}+\omega^2\frac{\partial\rho}{\partial z}w+2\frac{\partial}{\partial z}\left(\frac{\partial\mu}{\partial z}\frac{\partial w}{\partial z}\right)+\frac{\partial}{\partial z}\left(\frac{\partial\lambda}{\partial z}\Delta\right)=0\,. \tag{5.8}$$

Combining (5.7) and (5.8), we obtain

$$K\frac{\partial^2}{\partial x^2}\begin{pmatrix}\Delta\\ w\end{pmatrix}+L\begin{pmatrix}\Delta\\ w\end{pmatrix}=\begin{pmatrix}0\\ 0\end{pmatrix}, \tag{5.9}$$

where the matrices K and L contain depth operators.

The formulation of elasticity given by (5.6) and (5.7) does not factor due to the presence of terms involving a single x derivative. The approach of Section 2 may be generalized to solve (5.9), which is a vector wave equation that is in the same form as the scalar wave equation (2.3). Factoring (5.9) and retaining the outgoing factor, we obtain the outgoing elastic wave equation,

$$\frac{\partial}{\partial x}\begin{pmatrix}\Delta\\ w\end{pmatrix}=i\left(K^{-1}L\right)^{1/2}\begin{pmatrix}\Delta\\ w\end{pmatrix}. \tag{5.10}$$

Rearranging (5.10), we obtain

$$\frac{\partial}{\partial x}\begin{pmatrix}\Delta\\ w\end{pmatrix}=ik_0(I+X)^{1/2}\begin{pmatrix}\Delta\\ w\end{pmatrix}, \tag{5.11}$$

$$X=k_0^{-2}\left(K^{-1}L-k_0^2 I\right). \tag{5.12}$$

The operator square root in (5.11) is approximated using a rational function (Section 2) to obtain the elastic PE. The numerical solution of the elastic PE, which is similar to the numerical solution of the acoustic PE, is described in [14].

6. THE SPLIT-STEP PADÉ SOLUTION

The finite-difference solution of (2.7) is orders of magnitude faster than the finite-difference solution of (2.2). It is possible to achieve even greater efficiency with the split-step Padé solution [15], which is based on formally integrating (2.6) to obtain

$$p(r+\Delta r) = \exp\left[ik_0\Delta r\left(-1+\sqrt{1+X}\right)\right]p(r)\,, \tag{6.1}$$

where Δr is an arbitrary range step. Substituting a rational approximation for the exponential of the square root, we obtain

$$p(r+\Delta r) = \left(1+\sum_{j=1}^{n}\frac{\alpha_{j,n}X}{1+\beta_{j,n}X}\right)p(r)\,, \tag{6.2}$$

where the coefficients $\alpha_{j,n}$ and $\beta_{j,n}$ depend on Δr.

The split-step Padé solution allows large values of Δr because the rational approximation provides higher-order accuracy in both X and Δr. Another advantage of the split-step Padé solution is that the terms on the right side of (6.2) may be evaluated in parallel on a multi-processor computer. The finite-difference solution of (2.7) usually requires Δr to be less than a wavelength. For the split-step Padé solution, the only limitation on the size of Δr is the rate of range dependence. The split-step Padé solution typically provides an additional gain in efficiency of about two orders of magnitude. The split-step Padé solution has been generalized to allow dense sampling of the solution in range [16].

When the PE method was first applied to ocean acoustics [3], the split-step Fourier algorithm [32] was used to obtain numerical solutions. Although the applications of this approach are limited (e.g., it is not applicable to the higher-order PE or the elastic PE), it has remained in wide use due to an efficiency advantage over the finite-difference solution. The improved efficiency that the split-step Padé solution achieves (without sacrificing accuracy or capability) might be sufficient to overcome this advantage, especially for the shallow water problems that are currently of interest.

7. THE SELF-STARTER

To obtain a solution with the PE method, it is necessary to specify an initial condition corresponding to a source. An exact initial condition may be obtained by applying separation of

variables to solve (2.2). High-frequency approximations have been applied to develop more efficient starting fields [3,26,33]. The self-starter is an approach for obtaining an initial condition that provides both accuracy and efficiency and is based on the PE method (hence the name). In a mathematical sense, the self-starter is one of four applications of the PE method, which is applicable to approximating the wave equation in the interior of the domain [1-3], generating radiation boundary conditions [34,35], solving scattering problems [9,29], and generating initial conditions.

We derive the self-starter for the case of a line source in an ocean overlying an elastic bottom. Placing a source function on the right side of (5.9), we obtain

$$K\frac{\partial^2}{\partial x^2}\begin{pmatrix}\Delta\\ w\end{pmatrix}+L\begin{pmatrix}\Delta\\ w\end{pmatrix}=\begin{pmatrix}-2i\delta(x)\delta(z-z_0)\\ 0\end{pmatrix}, \tag{7.1}$$

where z_0 is in the water column. Integrating (7.1) over an arbitrarily small interval about $x = 0$, we obtain

$$\lim_{x\to 0^+} K\frac{\partial}{\partial x}\begin{pmatrix}\Delta\\ w\end{pmatrix}=\begin{pmatrix}-i\delta(z-z_0)\\ 0\end{pmatrix}. \tag{7.2}$$

Using (5.10) to replace the x derivative in (7.2), we obtain

$$\lim_{x\to 0^+} K\left(K^{-1}L\right)^{1/2}\begin{pmatrix}\Delta\\ w\end{pmatrix}=\begin{pmatrix}\delta(z-z_0)\\ 0\end{pmatrix}. \tag{7.3}$$

It is not possible to evaluate (7.3) numerically because the solution is singular at $z = z_0$.

We evaluate the field away from the origin to avoid the singularity. Applying the formal solution used in the derivation of the split-step Padé solution (Section 6), we obtain

$$\begin{pmatrix}\Delta\\ w\end{pmatrix}=\exp\left[ix\left(K^{-1}L\right)^{1/2}\right]\left(K^{-1}L\right)^{-1/2}K^{-1}\begin{pmatrix}\delta(z-z_0)\\ 0\end{pmatrix}. \tag{7.4}$$

Using the fact that an operator commutes with the exponential of itself, we rearrange (7.4) as

$$\begin{pmatrix}\Delta\\ w\end{pmatrix}=\left(K^{-1}L\right)^{1/2}\exp\left[ix\left(K^{-1}L\right)^{1/2}\right]L^{-1}\begin{pmatrix}\delta(z-z_0)\\ 0\end{pmatrix}. \tag{7.5}$$

No numerical difficulties are encountered when (7.5) is evaluated at $x = x_0$, where x_0 is on the order of a few wavelengths.

The first step in constructing the self-starter involves solving

$$L\begin{pmatrix}\Delta_{\mathrm{I}}\\ w_{\mathrm{I}}\end{pmatrix}=\begin{pmatrix}\delta(z-z_0)\\ 0\end{pmatrix}. \tag{7.6}$$

The bounded solution of this problem is then propagated out a short distance in range to $x = x_0$ using the elastic PE (Section 5) to obtain

$$\begin{pmatrix}\Delta_{\mathrm{II}}\\ w_{\mathrm{II}}\end{pmatrix}=\exp\left[ix_0\left(K^{-1}L\right)^{1/2}\right]\begin{pmatrix}\Delta_{\mathrm{I}}\\ w_{\mathrm{I}}\end{pmatrix}. \tag{7.7}$$

Finally, we apply a rational function to approximate the operator square root and obtain

$$\begin{pmatrix}\Delta\\ w\end{pmatrix}=\left(K^{-1}L\right)^{1/2}\begin{pmatrix}\Delta_{\mathrm{II}}\\ w_{\mathrm{II}}\end{pmatrix}. \tag{7.8}$$

In contrast to the starting fields that are based on high-frequency approximations, the self-starter depends on the depth-dependent properties of the medium and satisfies all interface and boundary conditions. The self-starter requires the solution of only a small number of boundary-value problems. To generate an initial condition in terms of the horizontal wave-number spectrum or normal modes, it is necessary to solve hundreds or thousands of similar boundary-value problems. The self-starter is applicable to problems involving fluid, elastic, and poro-elastic (Section 8) layers. With a minor modification that is described in [17], the self-starter may be applied to problems involving point sources. The self-starter is also applicable to problems involving compressional and shear sources in elastic [10] and poro-elastic [18] layers.

8. THE PORO-ELASTIC PE

In some cases, it is appropriate to treat ocean sediments as poro-elastic media [37-42], which support fast and slow compressional waves and shear waves. The density of the porous solid is denoted by ρ_s. The density of the fluid that occupies the pore spaces in denoted by ρ_f. The porosity α is the fraction of the medium (by volume) that consists of pore spaces. The other parameters that are required to describe a poro-elastic medium are the three wave speeds and attenuations and an added mass parameter that accounts for the geometry of the pore spaces [38-42]. It is necessary to numerically invert a nonlinear mapping to obtain the coefficients of the poro-elastic wave equation from these parameters [18].

As in Section 5, we obtain the equations of motion by applying $\mathbf{F} = m\mathbf{a}$ to a small volume element for the case of a line source. The x component of $\mathbf{F} = m\mathbf{a}$ for the combination of the solid and fluid components is

$$\frac{\partial\sigma_{xx}}{\partial x}+\frac{\partial\sigma_{xz}}{\partial z}=(1-\alpha)\rho_s\frac{\partial^2 u}{\partial t^2}+\alpha\rho_f\frac{\partial^2 u_f}{\partial t^2}, \tag{8.1}$$

where $\mathbf{u} = (u,v,w)$ is the displacement of the porous solid and $\mathbf{u}_f = (u_f, v_f, w_f)$ is the displacement of the fluid. The x component of $\mathbf{F} = m\mathbf{a}$ for the fluid component is

$$\frac{\partial \sigma}{\partial x} = \rho_f \frac{\partial^2 u_f}{\partial t^2} + \frac{\tau \rho_f}{\alpha} \frac{\partial^2 U}{\partial t^2} + \frac{\eta}{\kappa} \frac{\partial U}{\partial t}, \tag{8.2}$$

where $-\sigma$ is the fluid pressure and $\mathbf{U} = (U,V,W) = \alpha(\mathbf{u}_f - \mathbf{u})$. The terms involving the parameters τ, η, and κ account for the geometry of the pore spaces and Darcy's law for flow in porous media [37-43].

The constitutive equations (Hooke's law) [37-42] are

$$\sigma_{xx} = \lambda\Delta + 2\mu \frac{\partial u}{\partial x} + C\zeta, \tag{8.3}$$

$$\sigma_{zz} = \lambda\Delta + 2\mu \frac{\partial w}{\partial z} + C\zeta, \tag{8.4}$$

$$\sigma_{xz} = \mu\left(\frac{\partial u}{\partial z} + \frac{\partial w}{\partial x}\right), \tag{8.5}$$

$$\sigma = C\Delta + M\zeta, \tag{8.6}$$

where $\Delta = \nabla \cdot \mathbf{u}$, $\zeta = \nabla \cdot \mathbf{U}$, and λ, μ, C, and M are properties of the poro-elastic medium. These equations are generalizations of the constitutive equations for elastic media. For the time-harmonic problem, we substitute the constitutive equations into (8.1), (8.2), and similar equations for the z components of Newton's law to obtain the equations of motion,

$$\mu \frac{\partial^2 u}{\partial x^2} + \mu \frac{\partial^2 u}{\partial z^2} + \rho\omega^2 u + (\lambda + \mu)\frac{\partial \Delta}{\partial x} + \frac{\partial \mu}{\partial z}\frac{\partial u}{\partial z} + \frac{\partial \mu}{\partial z}\frac{\partial w}{\partial x} + C\frac{\partial \zeta}{\partial x} + \rho_f \omega^2 U = 0, \tag{8.7}$$

$$\mu \frac{\partial^2 w}{\partial x^2} + \mu \frac{\partial^2 w}{\partial z^2} + \rho\omega^2 w + (\lambda + \mu)\frac{\partial \Delta}{\partial z} + \frac{\partial \lambda}{\partial z}\Delta + 2\frac{\partial \mu}{\partial z}\frac{\partial w}{\partial z} + \frac{\partial}{\partial z}(C\zeta) + \rho_f \omega^2 W = 0, \tag{8.8}$$

$$C\frac{\partial \Delta}{\partial x} + M\frac{\partial \zeta}{\partial x} + \rho_f \omega^2 u + \rho_c \omega^2 U = 0, \tag{8.9}$$

$$\frac{\partial}{\partial z}(C\Delta) + \frac{\partial}{\partial z}(M\zeta) + \rho_f \omega^2 w + \rho_c \omega^2 W = 0, \tag{8.10}$$

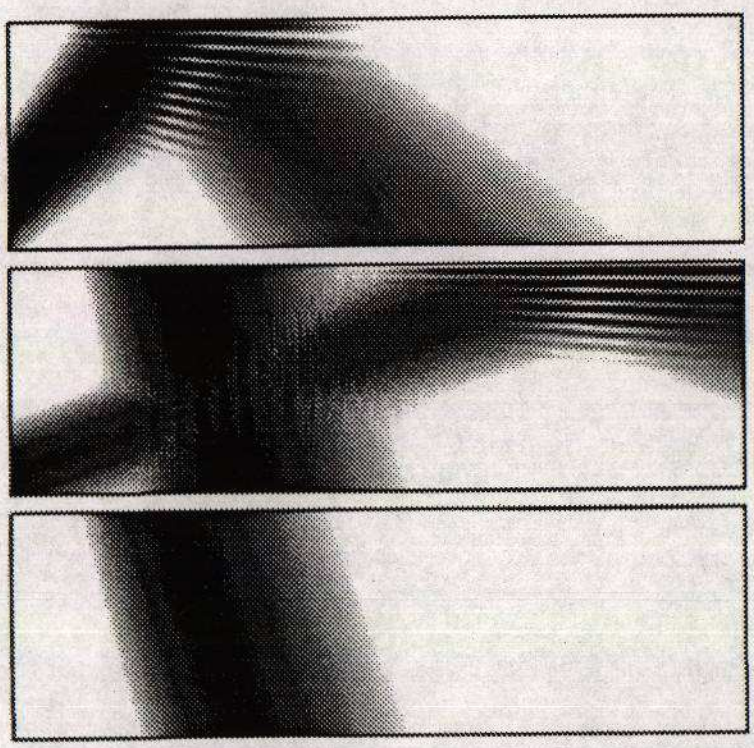

Figure 1. The poro-elastic PE solution for a 25-Hz problem involving a beamed array of compressional sources in a half space (Section 8). A fast wave radiates from the array and reflects from the boundary (top). Slow waves radiate from the array and the boundary (middle). A shear wave radiates from the boundary (bottom).

Figure 2. The adiabatic mode PE solution for a 1-Hz source placed at the location of the source used in the Heard Island Feasibility Test (Section 9). The shadow of Heard Island is broadened by azimuthal coupling. Acoustic energy reaches both coasts of North America. The computation covers the entire earth, including the continents.

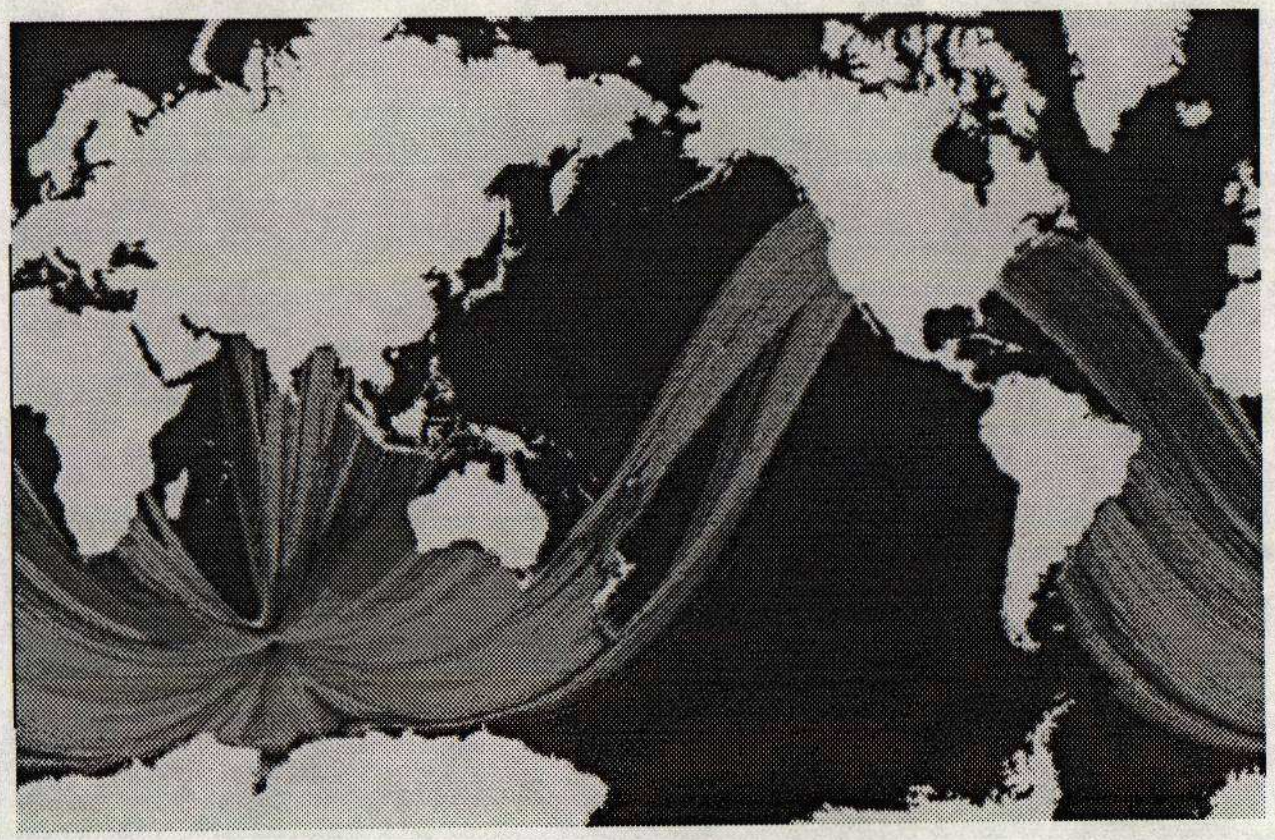

where $\rho = (1-\alpha)\rho_s + \alpha\rho_f$ and $\rho_c = \alpha^{-1}(1+\tau)\rho_f + i\omega^{-1}\kappa^{-1}\eta$. We have used slightly different notation than is used in the existing articles on poro-elasticity so that it is easy to see that (8.7) and (8.8) are generalizations of (5.6) and (5.7). The equations of motion are valid for problems involving piece-wise continuous depth variations in the poro-elastic parameters. These equations may be applied to problems involving fluid and elastic layers by applying the interface conditions described in [18].

Differentiating (8.7) with respect to x and (8.8) with respect to z and summing, we obtain

$$(\lambda+2\mu)\frac{\partial^2\Delta}{\partial x^2} + \frac{\partial}{\partial z}\left[(\lambda+2\mu)\frac{\partial\Delta}{\partial z}\right] + \rho\omega^2\Delta +$$

$$2\frac{\partial\mu}{\partial z}\frac{\partial^2 w}{\partial x^2} + \omega^2\frac{\partial\rho}{\partial z}w + 2\frac{\partial}{\partial z}\left(\frac{\partial\mu}{\partial z}\frac{\partial w}{\partial z}\right) + \frac{\partial}{\partial z}\left(\frac{\partial\lambda}{\partial z}\Delta\right) +$$

$$\rho_f\omega^2\zeta + C\frac{\partial^2\zeta}{\partial x^2} + \frac{\partial^2}{\partial z^2}(C\zeta) + \omega^2\frac{\partial\rho_f}{\partial z}W = 0\,. \tag{8.11}$$

This equation is a generalization of (5.8). Differentiating (8.9) with respect to x and (8.10) with respect to z and summing, we obtain

$$C\frac{\partial^2\Delta}{\partial x^2} + \frac{\partial^2}{\partial z^2}(C\Delta) + \rho_f\omega^2\Delta + M\frac{\partial^2\zeta}{\partial x^2} +$$

$$\frac{\partial^2}{\partial z^2}(M\zeta) + \rho_c\omega^2\zeta + \omega^2\frac{\partial\rho_f}{\partial z}w + \omega^2\frac{\partial\rho_c}{\partial z}W = 0\,. \tag{8.12}$$

Using (8.10) to eliminate W from (8.8), (8.11), and (8.12), we obtain the system of equations,

$$K\frac{\partial^2}{\partial x^2}\begin{pmatrix}\Delta\\ w\\ \zeta\end{pmatrix} + L\begin{pmatrix}\Delta\\ w\\ \zeta\end{pmatrix} = \begin{pmatrix}0\\ 0\\ 0\end{pmatrix}, \tag{8.13}$$

where the matrices K and L are generalized from the elastic case. This equation factors and may therefore be solved with the approach that is used to solve (5.9). For two-dimensional problems, the standard formulation of poro-elasticity involves four coupled equations. Since (8.13) involves only three equations, the standard formulation contains a redundant equation.

We illustrate the poro-elastic PE for a problem involving an array of 25-Hz sources in an idealized half space in which there is no attenuation, the fast wave speed is 2400 m / s, the slow wave speed is 1000 m / s, and the shear wave speed is 1200 m / s. The source array is phased so that the fast wave is incident on the boundary at 55 degrees from normal incidence. The source spacing is 20 m, with the top source 1 km from the boundary. The fast, slow, and shear potentials appear in

Figure 1. A fast wave radiates from the array and reflects from the boundary. A slow wave radiates from the array at a shallower angle due to its lower speed. Slow and shear waves radiate from the boundary due to coupling of energy when the fast wave is reflected.

9. THE ADIABATIC MODE PE

Like the PE method, the adiabatic mode solution [44,45] is efficient for range-dependent problems. This solution is based on the assumption that energy does not couple between modes in a gradually range-dependent medium (the PE method accounts for mode coupling). The normal-mode representation of the solution of (2.1) is

$$p = \sum p_j(r,\theta)\phi_j(z;r,\theta)\,, \tag{9.1}$$

$$\rho\frac{\partial}{\partial z}\left(\frac{1}{\rho}\frac{\partial\phi_j}{\partial z}\right)+k^2\phi_j = k_j^2(r,\theta)\phi_j\,, \tag{9.2}$$

where the ϕ_j and k_j are the normal modes and eigenvalues and the p_j are to be determined. The semicolon in the argument of ϕ_j indicates gradual variation with r and θ.

Substituting (9.1) into (2.1) and neglecting mode coupling, we obtain

$$\frac{\partial^2 p_j}{\partial r^2}+\frac{1}{r^2}\frac{\partial^2 p_j}{\partial\theta^2}+k_j^2 p_j = 0\,. \tag{9.3}$$

Factoring (9.3) and assuming that back-scattered energy may be neglected, we obtain the outgoing wave equation,

$$\frac{\partial p_j}{\partial r} = i\left(\frac{1}{r^2}\frac{\partial^2}{\partial\theta^2}+k_j^2\right)^{1/2} p_j\,, \tag{9.4}$$

which may be solved using the approach described in Section 2. The factorization of (9.3) is not exact because the operator in the square root depends on r. The factorization is an accurate approximation, however, because the azimuthal term varies slowly with r in the farfield. By reducing a three-dimensional problem to a small number of two-dimensional problems, it becomes practical to solve large-scale problems. A simple correction that accounts for the curvature of the waveguide is incorporated into (9.4) for global-scale problems [19].

We illustrate the adiabatic mode PE for a problem involving a 1-Hz source at 74.5° E and 53.4° S, which is the location of the source used in the Heard Island Feasibility Test [46]. The energy in the first mode is displayed in Figure 2. Since the horizontal phase speed is higher in

shallow water, energy is deflected away from shallow water by horizontal refraction. This effect causes Heard Island to cast a broad shadow to the north-northwest of the source.

10. THE WINDY PE

The adiabatic mode PE has been extended to account for the effects of fluid flow and applied to model acoustic propagation from the impact sites of the fragments of Comet Shoemaker-Levy 9 [21]. We define the sound speed c, the wind velocity $\mathbf{u} = (u_r, u_\theta, u_z)$, and the acoustic velocity $\mathbf{v} = (v_r, v_\theta, v_z)$. We neglect the vertical component of the wind, which is assumed to be dominated by the horizontal components. As in [47], we assume that variations in the properties of the medium are gradual temporally with respect to a representative acoustic period and spatially with respect to a representative acoustic wavelength. We also assume that horizontal variations are more gradual than vertical variations. Under these assumptions, the formulation of [47] reduces to

$$D_t \mathbf{v} + \frac{1}{\rho} \nabla p = 0 , \tag{10.1}$$

$$\frac{\partial^2 p}{\partial r^2} + \frac{1}{r^2} \frac{\partial^2 p}{\partial \theta^2} + \rho \left(\frac{1}{\rho} \frac{\partial p}{\partial z} \right) - \frac{1}{c^2} D_t^2 p + 2\rho \frac{\partial u_r}{\partial z} \frac{\partial v_z}{\partial r} + \frac{2\rho}{r} \frac{\partial u_\theta}{\partial z} \frac{\partial v_z}{\partial \theta} = 0 , \tag{10.2}$$

where

$$D_t = \frac{\partial}{\partial t} + \mathbf{u} \cdot \nabla . \tag{10.3}$$

For the time-harmonic problem, we assume that $\varepsilon \ll 1$, where $\varepsilon = \left| c^{-1} \mathbf{u} \right|$ is the Mach number, and obtain

$$\mathbf{v} = -\frac{i}{\omega \rho} \nabla p + O(\varepsilon) , \tag{10.4}$$

$$D_t = -i\omega + \mathbf{u} \cdot \nabla , \tag{10.5}$$

$$D_t^2 = -\omega^2 - 2i\omega \mathbf{u} \cdot \nabla + O\left(\varepsilon^2\right) , \tag{10.6}$$

and (10.2) reduces to

$$\frac{\partial^2 p}{\partial r^2} + \frac{2iku_r}{c} \frac{\partial p}{\partial r} + \frac{1}{r^2} \frac{\partial^2 p}{\partial \theta^2} + \frac{2iku_\theta}{rc} \frac{\partial p}{\partial \theta} + \rho \frac{\partial}{\partial z} \left(\frac{1}{\rho} \frac{\partial p}{\partial z} \right) + k^2 p - \frac{2i}{\omega} \frac{\partial u_r}{\partial z} \frac{\partial^2 p}{\partial r \partial z} - \frac{2i}{r\omega} \frac{\partial u_\theta}{\partial z} \frac{\partial^2 p}{\partial \theta \partial z} = O\left(\varepsilon^2\right) . \tag{10.7}$$

Figure 3. The windy PE solution of a Jovian acoustics problem involving a 2-mHz source at the location of the impact site of Comet Shoemaker-Levy 9 (Section 10). An intense beam of energy radiates from the impact site toward the west. This beam is formed by refraction due to wind shear in the cloud belts. This effect also gives rise to several weaker beams.

Figure 4. PE solution for a problem involving a 25-Hz source located 12.5 km from the beach in a 200-m deep region of the water column (Section 11). The ocean bottom consists of a sediment that is 100 m thick and runs parallel to the upper boundary. A basement half space lies below the sediment layer.

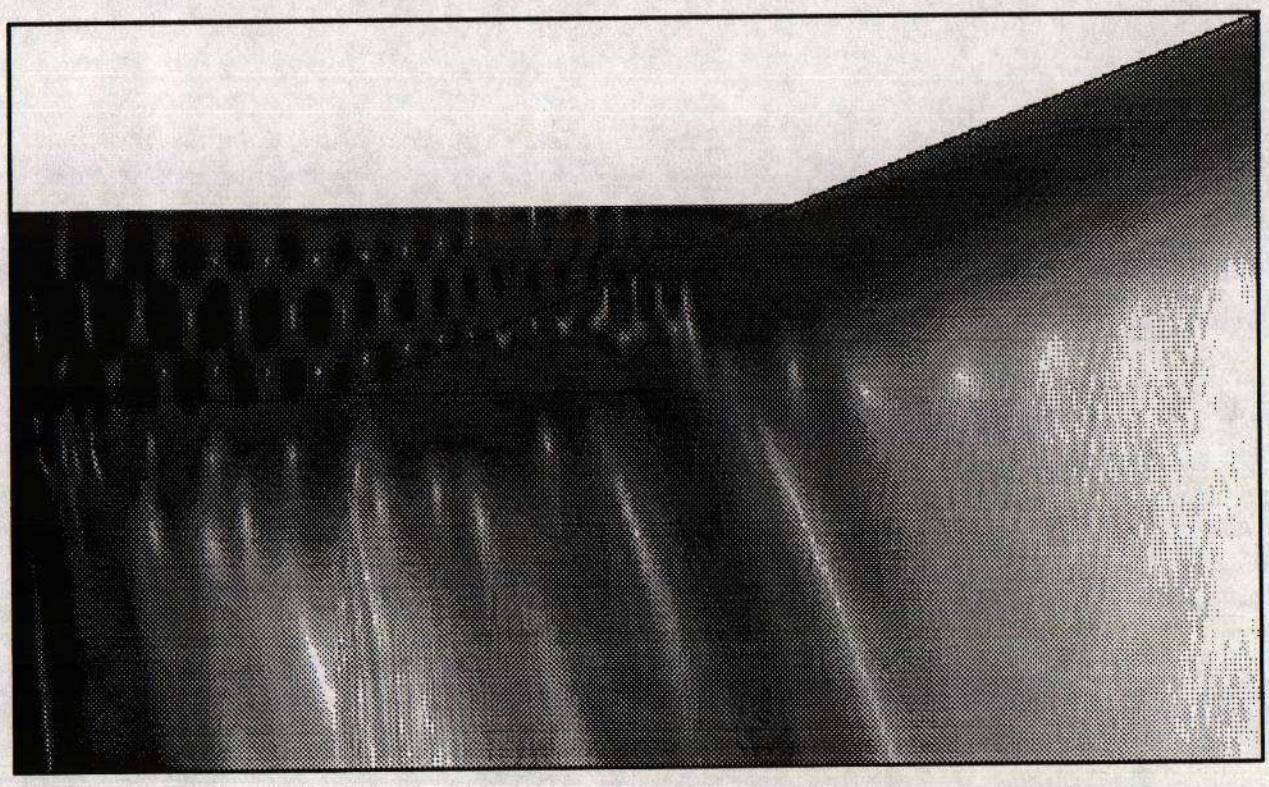

The following generalization of (9.3) is correct to $O(\varepsilon)$ when energy coupling between modes is negligible [21]:

$$\frac{\partial^2 p_j}{\partial r^2} + 2iw_r \frac{\partial p_j}{\partial r} + \frac{1}{r^2}\frac{\partial^2 p_j}{\partial \theta^2} + \frac{2iw_\theta}{r}\frac{\partial p_j}{\partial \theta} + k_j^2 p_j = 0\,, \tag{10.8}$$

where w_r and w_θ are the r and θ components of

$$\mathbf{w} = \int \frac{1}{\rho}\phi_j \left(\frac{\mathbf{k}\mathbf{u}\phi_j}{c} - \frac{1}{\omega}\frac{\partial \mathbf{u}}{\partial z}\frac{\partial \phi_j}{\partial z} \right) dz\,. \tag{10.9}$$

Since $|w_r|^2 \ll |w_r|$, (10.8) is asymptotically equivalent to

$$\left(\frac{\partial}{\partial r} + iw_r \right)^2 p_j + \frac{1}{r^2}\frac{\partial^2 p_j}{\partial \theta^2} + \frac{2iw_\theta}{r}\frac{\partial p_j}{\partial \theta} + k_j^2 p_j = 0\,. \tag{10.10}$$

We use the assumption of gradual horizontal variations to factor (10.10) and obtain the outgoing wave equation,

$$\frac{\partial p_j}{\partial r} = -iw_r p_j + i\left(\frac{1}{r^2}\frac{\partial^2}{\partial \theta^2} + \frac{2iw_\theta}{r}\frac{\partial}{\partial \theta} + k_j^2 \right)^{1/2} p_j\,. \tag{10.11}$$

A simple correction that accounts for the curvature of the waveguide is incorporated into (10.11) for global-scale problems [19]. A related equation has been obtained for two-dimensional problems [48].

We apply the windy PE to model the propagation of a 2-mHz mode corresponding to a horizontal phase speed of 900 m / s from the impact sites of the fragments of Comet Shoemaker-Levy 9 [49-52]. Predictions for the prospects of detecting the impacts ranged from bleak [53] to favorable [54,55]. Fortunately, the optimistic predictions turned out to be correct [56-59]. Although several types of wave propagation from the impact sites were modeled [60-65], little attention was given to the problem of acoustic propagation in the sound channel, which is a layer of low sound speed that is analogous to the sound channel in the ocean [66]. We decided to model this problem because the comet was expected to (and apparently did) explode within the sound channel [54,55].

The depth dependence of the sound speed [67] and the latitudinal dependence of the zonal winds [68] are known from Voyager data. The geographic dependence of the sound speed is not known but is not expected to be a major factor. The zonal winds blow in different directions at different latitudes with speeds of over 160 m / s near the equator and peak speeds of about 40 m / s near the impact latitude of 44° S. The cells that lie between wind reversals correspond roughly to the Jovian cloud belts. Acoustic energy gets refracted by wind shear in these belts, which are acoustic waveguides. As the results in Figure 3 indicate, some of these waveguides pinch the energy

radiating from the impact site into intense beams that remain coherent for long distances. We have confirmed this behavior with ray solutions. Since the beams are formed by geometric effects, they occur for all modes and all frequencies in a wide band. The beams should therefore be the most prominent acoustic features away from the impact sites. Since acoustic waves were detected near the impact sites in raw data, there is a chance that the beams will be detected in processed data.

11. TAPERING WAVEGUIDES

The PE method can be used to solve problems involving waveguides of varying thickness, with applications to beach acoustics [22]. When the location of the upper boundary of the waveguide varies with range, the PE method may be implemented using the approach that was used for the rotated PE [69]. As in Section 2, the environment is approximated by a sequence of stratified regions, and the upper boundary becomes a sequence of stair steps. The pressure-release boundary condition $p = 0$ is applied along the runs of the steps. The depth operator in (2.7) is approximated using finite differences, and the vertical interfaces between regions are handled by adding and subtracting grid points as the location of the upper boundary varies.

We apply this approach to a problem involving propagation from the ocean onto the beach. A 25-Hz source is placed in a 200-m deep water column 12.5 km from the beach. The ocean bottom consists of a 100-m thick sediment layer overlying a basement half space. The sound speed is 1500 m / s in the water, 1704.5 m / s in the sediment, and 1850 m / s in the basement. The density is 1.15 g / cm^3 in the sediment and 1.5 g / cm^3 in the basement. The attenuation (in decibels per wavelength) is 0.1 in the sediment and 0.25 in the basement. The results in Figure 4 indicate that three modes are excited in the water column and that a significant amount of energy couples into the sediment layer and propagates several kilometers inland. Beyond the beach, the transmission loss levels in the sediment range from about 60 to 90 dB.

12. SUMMARY

The PE method has recently undergone improvements in accuracy (Sections 2,3,7), capability (Sections 4,5,7,8,10,11), and efficiency (Sections 6,7,9). The higher-order energy-conserving PE is accurate when the uncoupled azimuth approximation is valid and the sediment may be modeled as a fluid. Complete energy-conservation corrections need to be developed for the elastic PE and the poro-elastic PE, which are accurate when the environment varies gradually with range. The self-starter is an accurate and efficient technique for generating initial conditions. The split-step Padé solution is orders of magnitude faster than other algorithms for solving the higher-order PE and the elastic PE. The adiabatic mode PE is an efficient approach for investigating three-dimensional effects. The windy PE is a generalization of the adiabatic mode PE that is useful for solving problems in Jovian acoustics. The PE method has also been generalized to handle problems involving waveguides of variable thickness.

13. ACKNOWLEDGMENTS

This work was supported by the Office of Naval Research. The author thanks his collaborators, whose names appear in several of the references. Special thanks go to W.A. Kuperman for his support.

14. REFERENCES

[1] M.A. Leontovich and V.A. Fock, "Solution of the problem of propagation of electromagnetic waves along the earth's surface by the method of parabolic equation," J. Exp. Theor. Phys. 16, 557-573 (1946).
[2] V.A. Fock, *Electromagnetic Diffraction and Propagation Problems* (Pergamon, New York, 1965), pp. 213-234.
[3] F.D. Tappert, "The parabolic approximation method," in *Wave Propagation and Underwater Acoustics*, edited by J.B. Keller and J.S. Papadakis, Lecture Notes in Physics, Vol. 70 (Springer, New York, 1977).
[4] A. Bamberger, B. Engquist, L. Halpern, and P. Joly, "Higher order paraxial wave equation approximations in heterogeneous media," SIAM J. Appl. Math. 48, 129-154 (1988).
[5] M.D. Collins, "Applications and time-domain solution of higher-order parabolic equations in underwater acoustics," J. Acoust. Soc. Am. 86, 1097-1102 (1989).
[6] M.B. Porter, F.B. Jensen, and C.M. Ferla, "The problem of energy conservation in one-way models," J. Acoust. Soc. Am. 89, 1058-1067 (1991).
[7] M.D. Collins and E.K. Westwood, "A higher-order energy-conserving parabolic equation for range-dependent ocean depth, sound speed, and density," J. Acoust. Soc. Am. 89, 1068-1075 (1991).
[8] M.D. Collins, "An energy-conserving parabolic equation for elastic media," J. Acoust. Soc. Am. 94, 975-982 (1993).
[9] M.D. Collins and R.B. Evans, "A two-way parabolic equation for acoustic back scattering in the ocean," J. Acoust. Soc. Am. 91, 1357-1368 (1992).
[10] M.D. Collins, "A two-way parabolic equation for elastic media," J. Acoust. Soc. Am. 93, 1815-1825 (1993).
[11] R.R. Greene, "A high-angle one-way wave equation for seismic wave propagation along rough and sloping interfaces," J. Acoust. Soc. Am. 77, 1991-1998 (1985).
[12] M.D. Collins, "A higher-order parabolic equation for wave propagation in an ocean overlying an elastic bottom," J. Acoust. Soc. Am. 86, 1459-1464 (1989).
[13] B.T.R. Wetton and G.H. Brooke, "One-way wave equations for seismoacoustic propagation in elastic waveguides," J. Acoust. Soc. Am. 87, 624-632 (1990).
[14] M.D. Collins, "Higher-order parabolic approximations for accurate and stable elastic parabolic equations with application to interface wave propagation," J. Acoust. Soc. Am. 89, 1050-1057 (1991).
[15] M.D. Collins, "A split-step Padé solution for parabolic equation method," J. Acoust. Soc. Am. 93, 1736-1742 (1993).
[16] M.D. Collins, "Generalization of the split-step Padé solution," J. Acoust. Soc. Am. 96, 382-385 (1994).
[17] M.D. Collins, "A self-starter for the parabolic equation method," J. Acoust. Soc. Am. 92, 1357-1368 (1992).
[18] M.D. Collins, W.A. Kuperman, and W.L. Siegmann, "A parabolic equation for poro-elastic media," J. Acoust. Soc. Am. (in press).

[19] M.D. Collins, "The adiabatic mode parabolic equation," J. Acoust. Soc. Am. 94, 2269-2278 (1993).
[20] M.D. Collins, B.E. McDonald, K.D. Heaney, and W.A. Kuperman, "Three-dimensional effects in global acoustics," J. Acoust. Soc. Am. (in press).
[21] M.D. Collins, B.E. McDonald, W.A. Kuperman, and W.L. Siegmann, "Jovian acoustics and Comet Shoemaker-Levy 9," J. Acoust. Soc. Am. (in press).
[22] M.D. Collins, R.A. Coury, and W.L. Siegmann, "Beach acoustics," J. Acoust. Soc. Am. (in press).
[23] J.S. Perkins and R.N. Baer, "An approximation to the three-dimensional parabolic-equation method for acoustic propagation," J. Acoust. Soc. Am. 72, 515-522 (1982).
[24] J.F. Claerbout, *Fundamentals of Geophysical Data Processing* (McGraw-Hill, New York, 1976), pp. 206-207.
[25] G. Botseas, D. Lee, and K.E. Gilbert, "IFD: Wide-angle capability," Naval Underwater Systems Center, Technical Report 6905 (New London, Connecticut, 1983).
[26] R.R. Greene, "The rational approximation to the acoustic wave equation with bottom interaction," J. Acoust. Soc. Am. 76, 1764-1773 (1984).
[27] F.B. Jensen and C.M. Ferla, "Numerical solutions of range-dependent benchmark problems," J. Acoust. Soc. Am. 87, 1499-1510 (1990).
[28] H. Bremmer, "The W.K.B. approximation as the first term of a geometric-optical series," Comm. Pure and Appl. Math. 4, 105-115 (1951).
[29] G.A. Kriegsmann, A. Taflove, and K.R. Umashankar, "A new formulation of electromagnetic wave scattering using an on-surface radiation boundary condition approach," IEEE Trans. Ant. and Prop. 35, 153-161 (1987).
[30] G.A. Kriegsmann and P.G. Petropolis, "An approximate method for the study of transverse discontinuities in waveguides," Wave Motion 13, 123-131 (1991).
[31] H. Kolsky, *Stress Waves in Solids* (Dover, New York, 1963), pp. 10-11.
[32] S.M. Flatté and F.D. Tappert, "Calculation of the effect of internal waves on oceanic sound transmission," J. Acoust. Soc. Am. 58, 1151-1159 (1975).
[33] M.D. Collins, "A nearfield asymptotic analysis for underwater acoustics," J. Acoust. Soc. Am. 85, 1107-1114 (1989).
[34] B. Engquist and A. Majda, "Absorbing boundary conditions for the numerical simulation of waves," Math. Comp. 31, 629-651 (1977).
[35] R.W. Clayton and B. Engquist, "Absorbing boundary conditions for wave-equation migration," Geophysics 45, 895-904 (1980).
[36] M.A. Biot, "Theory of propagation of elastic waves in a fluid-saturated porous solid," J. Acoust. Soc. Am. 28, 168-191 (1956).
[37] M.A. Biot, "Generalized theory of acoustic propagation in porous dissipative media," J. Acoust. Soc. Am. 34, 1254-1264 (1962).
[38] R.D. Stoll and T.K. Kan, "Reflection of acoustic waves at a water-sediment interface," J. Acoust. Soc. Am. 70, 149-156 (1981).
[39] T. Yamamoto, "Acoustic propagation in the ocean with a poro-elastic bottom," J. Acoust. Soc. Am. 73, 1587-1596 (1983).
[40] M. Stern, A. Bedford, and H.R. Millwater, "Wave reflection from a sediment layer with depth-dependent properties," J. Acoust. Soc. Am. 77, 1781-1788 (1985).
[41] D.G. Albert, "A comparison between wave propagation in water-saturated and air-saturated porous materials," J. Appl. Phys. 73, 28-36 (1993).
[42] M. Badiey, I. Jaya, and A.H-D. Cheng, "Propagator matrix for plane wave reflection from inhomogeneous anisotropic poroelastic seafloor," J. Comp. Acoust. 2, 11-27 (1994).
[43] C.S. Yih, *Fluid Mechanics* (West River Press, Ann Arbor, 1977), p. 379.

[44] A.D. Pierce, "Extension of the method of normal modes to sound propagation in an almost-stratified medium," J. Acoust. Soc. Am. 37, 19-27 (1965).
[45] H. Weinberg and R. Burridge, "Horizontal ray theory for ocean acoustics," J. Acoust. Soc. Am. 55, 63-79 (1974).
[46] A.B. Baggeroer and W. Munk, "The Heard Island Feasibility Test," *Physics Today* 45(9), 22-30 (1992).
[47] A.D. Pierce, "Wave equation for sound in fluids with unsteady inhomogeneous flow," J. Acoust. Soc. Am. 87, 2292-2299 (1990).
[48] J.S. Robertson, W.L. Siegmann, and M.J. Jacobson, "Current and current shear effects in the parabolic approximation for underwater sound channels," J. Acoust. Soc. Am. 77, 1768-1780 (1985).
[49] C.S. Shoemaker, E.M. Shoemaker, and D.H. Levy, IAU Circ. 5725 (1993).
[50] C.R. Chapman, "Comet on target for Jupiter," Nature 363, 492-493 (1993).
[51] J.K. Beatty and D.H. Levy, "Awaiting the crash," Sky & Telescope 87(1), 40-44 (1994).
[52] J.K. Beatty and D.H. Levy, "Awaiting the crash—Part II," Sky & Telescope 88(1), 18-23 (1994).
[53] P. Weissman, "The big fizzle is coming," Nature 370, 94 (1994).
[54] K. Zahnle and M.-M. Mac Low, "The collision of Jupiter and Comet Shoemaker-Levy 9," Icarus 108, 1-17 (1994).
[55] T.J. Ahrens, T. Takata, J.D. O'Keefe, and G.S. Orton, "Impact of Comet Shoemaker-Levy 9 on Jupiter," Geophys. Res. Lett. 21, 1087-1090 (1994).
[56] R.A. Kerr, "Shoemaker-Levy dazzles, bewilders," Science 363, 492-493 (1994).
[57] C.R. Chapman, "Dazzling demise of a comet," Nature 370, 245-246 (1994).
[58] J.K. Beatty and S.J. Goldman, "The great crash of 1994: A first report," Sky & Telescope 88(4), 18-23 (1994).
[59] S.J. O'Meara, "The great dark spots of Jupiter," Sky & Telescope 88(5), 30-35 (1994).
[60] J. Harrington, R.P. LeBeau, K.A. Backes, and T.E. Dowling, "Dynamic response of Jupiter's atmosphere to the impact of Comet Shoemaker-Levy 9," Nature 368, 525-527 (1994).
[61] M.S. Marley, "Seismological consequences of the collision of Shoemaker-Levy/9 with Jupiter," Astrophys. Jour. Lett. 427, 63-66 (1994).
[62] U. Lee and H.M. Van Horn, "Global oscillation amplitudes excited by the Jupiter-Comet collision," Astrophys. Jour. Lett. 428, 41-44 (1994).
[63] A.P. Ingersoll, H. Kanamori, and T.E. Dowling, "Atmospheric gravity waves from the impact of Comet Shoemaker-Levy 9 with Jupiter," Geophys. Res. Lett. 21, 1083-1086 (1994).
[64] D.M. Hunten, W.F. Hoffman, and A.L. Sprague, "Jovian seismic waves and their detection," Geophys. Res. Lett. 21, 1091-1094 (1994).
[65] D. Deming, "Prospects for Jovian seismological observations following the impact of Comet Shoemaker-Levy 9," Geophys. Res. Lett. 21, 1095-1098 (1994).
[66] W.H. Munk, "Sound channel in an exponentially stratified ocean with application to SOFAR", J. Acoust. Soc. Am. 55, 220-226 (1974).
[67] G.F. Lindal, G.E. Wood, G.S. Levy, J.D. Anderson, D.N. Sweetnam, H.B. Hotz, B.J. Buckles, D.P. Holmes, P.E. Doms, V.R. Eshleman, G.L. Tyler, and T.A. Croft, "The atmosphere of Jupiter: An analysis of the Voyager Radio Occultation Measurements", J. Geophys. Res. 86, 8721-8727 (1981).
[68] S.S. Limaye, "Jupiter: New estimates of the mean zonal flow at the cloud level", Icarus 65, 335-352 (1986).
[69] M.D. Collins, "The rotated parabolic equation and sloping ocean bottoms," J. Acoust. Soc. Am. 87, 1035-1037 (1990).